ORGANIC CHEMISTRY FRONTIERS

CCS 中国化学会 CHINESE CHEMICAL SOCIETY

SIOC 1950

ROYAL SOCIETY OF CHEMISTRY

RESEARCH ARTICLE

View Article Online
View Journal | View Issue

Cite this: *Org. Chem. Front.*, 2024, **11**, 1941

A convergent paired electrochemical strategy for decarboxylative C(sp^2)–C(sp^3) bond formation†

Lingjiao Li,‡[a,b] Zijian Li, ‡[b,c] Wenxuan Sun[a,b] and Chao Li *[a,b]

Received 31st December 2023,
Accepted 5th February 2024

DOI: 10.1039/d3qo02141f

rsc.li/frontiers-organic

In this report, we describe a convergent paired electrochemical decarboxylative C(sp^2)–C(sp^3) cross-coupling reaction that employs readily available alkyl carboxylic acids and C(sp^2)–iodides as direct coupling partners. This easy-to-operate electrochemical process occurs under mild conditions, uses inexpensive materials and reagents, requires no prefunctionalization of the native acids, and operates broadly across diverse aryl, heteroaryl, and alkenyl iodides, thereby providing powerful and flexible access to the construction of C(sp^2)–C(sp^3) bonds. The utility and practicality of this convergent paired electrolysis is demonstrated in the syntheses of high-value and synthetically challenging unnatural amino acids and terpenoid natural products. Extensive mechanistic studies shed light on the anodic PPh_3/NaI-mediated generation of *N*-hydroxyphthalimide esters and the cathodic reductive cross-coupling processes facilitated by Ni^I species.

Introduction

Over the last decade, decarboxylative C(sp^2)–C(sp^3) cross-coupling reactions that directly employ readily available aryl/vinyl halides as one of the coupling partners have been propelled to the forefront for C(sp^2)–C(sp^3) bond formation.[1] These appealing synthetic methods can be classified into 2 types of reactions (Fig. 1A): (1) metallaphotoredox cross-coupling, wherein an unmodified carboxylic acid is used directly and for which the homolytic cleavage of a C–CO_2H bond is achieved by photomediated single-electron oxidation;[2] (2) cross-electrophilic coupling (XEC), wherein a carboxylic acid is initially converted to a redox-active ester (RAE) that can abstract an electron from the low valent Ni catalyst generated in reductive conditions or from the reductants directly, driving decarboxylation of the RAE.[3–6] Recently, Fu's group reported innovative electrophotochemical Ce/Ni dual transition metal-catalyzed decarboxylative arylation and alkenylation reactions by integrating the photooxidation of carboxylic acids by anodic generated Ce^{IV} with cathodic nickel-catalyzed reductive cross-coupling.[7]

Despite significant advancements, several limitations persist in many reported decarboxylative C(sp^2)–C(sp^3) cross-

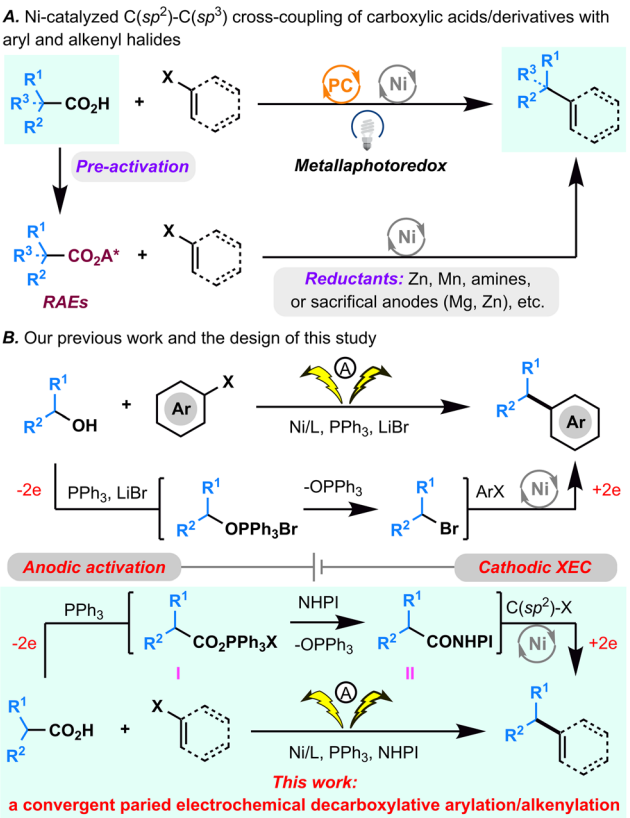

Fig. 1 (A) Established decarboxylative arylation/alkenylation strategies. (B) Our previous study on electrochemical dehydroxylative arylation and the envisioned convergent paired electrolysis for the decarboxylative arylation and alkenylation.

[a]*Tsinghua Institute of Multidisciplinary Biomedical Research, Tsinghua University, Beijing, 100084, China. E-mail: lichao@nibs.ac.cn*
[b]*National Institute of Biological Sciences, Beijing, 102206, China*
[c]*Academy for Advanced Interdisciplinary Studies, Peking University, Beijing 100871, China*

†Electronic supplementary information (ESI) available. See DOI: https://doi.org/10.1039/d3qo02141f

‡These authors contributed equally.

coupling reactions. Notably, the high oxidative potential of carboxylic acids poses constraints on oxidative decarboxylative cross-couplings, limiting their applicability in the presence of certain oxidation-sensitive functional groups when exposed to photoexcited catalysts. Additionally, reductive approaches often necessitate the preactivation of carboxylic acids (*e.g.*, separate preparation of RAEs) and the use of superstoichiometric reductants (*e.g.*, Zn, Mn, or sacrificial anodes). To address these challenges, we pursued a convergent paired electrochemical decarboxylative C(sp^2)–C(sp^3) cross-coupling reaction by seamlessly merging the anodic generation of RAEs with cathodic nickel-catalyzed reductive cross-coupling.

Previously, we devised a convergent paired electrochemical strategy for the dehydroxylative C(sp^2)–C(sp^3) bond formation (Fig. 1B).[8] In that approach, an unmodified alkyl alcohol underwent conversion to an alkyl bromide through an Appel reaction with anodic generated $PPh_3{\cdot}Br_2$, subsequently paired with Ni-catalyzed cathodic reductive cross-coupling to achieve formal dehydroxylative C(sp^2)–C(sp^3) bond formation. Building on this foundation, the current study explores the potential of anodically generated $PPh_3{\cdot}Br_2$ to activate carboxylic acids,[9,10] yielding acyloxytriphenylphosphonium ions. In the presence of NHPI, these ions are envisioned to be subsequently transformed into NHPI esters.[11] The integration of this process with cathodic decarboxylative cross-electrophilic coupling (XEC) aims to achieve formal direct decarboxylative C(sp^2)–C(sp^3) cross-coupling (Fig. 1B). However, given the inherent challenges associated with transition metal-catalyzed convergent paired electrolysis,[12] two critical considerations emerge: ensuring the harmonization of the intrinsic redox properties of all reactants and coordinating the reaction rates of the anodic $PPh_3{\cdot}Br_2$ generation, the acyloxytriphenylphosphonium ion and the NHPI ester formation, and the Ni catalytic cycle.

Results and discussion

We implemented this idea in practice by evaluating a series of electrochemical conditions using with 4-phenylbutyric acid (**1**) and iodobenzene (**2**) as model substrates (Table 1). After extensive optimization, the desired product **3** was obtained in 87% yield by running the electrolysis in a simple undivided cell under a constant current of 3 mA and using $NiBr_2{\cdot}$glyme as the precatalyst, 2,2′-bipyridine as the ligand, PPh_3, DMAP, and NHPI as activating agents, graphite as the anode, Ni foam as the cathode, NaI as the electrolyte, and NMP as the solvent, each of which was found to be required to obtain **3** in high yield (entries 1–7). Notably, all reagents and materials employed in this electrolysis are cost-effective and readily available. It is noteworthy that, interestingly, even in the absence of NaI, coupling products were obtained with a commendable 79% yield, without encountering high electrical resistance. This observation suggests that the salt generated from the carboxylic acid and DMAP effectively served as the electrolyte.[13] Beyond its role as a base, DMAP may also function as an acyl transfer reagent in the NHPI ester formation. This is evidenced

Table 1 Optimization of the electrochemical decarboxylative arylation[a]

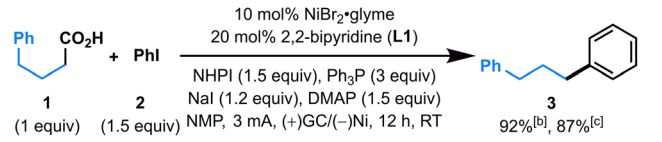

Entry	Deviation from above	Yield[b] (%)	Entry	Deviation from above	Yield[b] (%)
1	No electricity	0	8	$LiCO_4$ instead of NaI	78
2	w/o $NiBr_2{\cdot}$glyme	0	9	LiBr instead of NaI	74
3	w/o **L1**	5	10	**L2** instead of **L1**	74
4	w/o NHPI	0	11	**L3** instead of **L1**	55
5	w/o Ph_3P	0	12	Et_3N instead of DMAP	61
6	w/o DMAP	9	13	Pyridine instead of DMAP	30
7	w/o NaI	79	14	PhBr instead of PhI	33

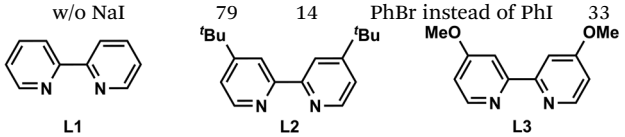

[a] Reactions were conducted on a 0.2 mmol scale in NMP (4 mL). [b] Yields were determined by GC/MS. [c] Yield of the isolated product.

by lower yields when replaced with Et_3N or pyridine (entries 12 and 13). Furthermore, the utilization of aryl iodide is imperative; substituting it with bromobenzene led to a reduced yield of 33% (entry 14).

With the optimized conditions in hand, we first examined the scope of aryl iodides (Fig. 2). Gratifyingly, we found that aryl iodides containing various functional groups at the *para*, *meta*, and *ortho* positions (**4–14**) were generally well accommodated in this convergent paired electrochemical decarboxylative arylation. Electron-poor (**4**, **5**, **9**, **12**, **19**), electron-neutral (**10**, **13**, **20**), and electron-rich (**6–8**, **11**, **14**, **21**) aryl iodides were all coupled with equal levels of efficiency, affording the desired products in good-to-high yields. Moreover, this reaction showed notable chemoselectivity toward aryl–I bonds, and a range of bromides and chlorides containing aryl fragments (**15**, **17**, **18**, **24**, **29**, **30**) were tolerated in this convergent paired electrolysis, allowing for further downstream diversification. Notably, a series of medicinally relevant and structurally distinct heterocycles including a quinoline (**22**), an unprotected indole (**23**), pyridines with various substitution patterns (**24–31**), a dibenzofuran (**32**), a carbazole (**33**), and a thiophene (**34**), were also investigated and the desired coupling products were successfully afforded in good-to-high yields.

We subsequently explored the substrate scope for carboxylic acid coupling partners (Fig. 2A and B). Overall, a range of primary and secondary carboxylic acids bearing a variety of functionalities, including ethers (**36**, **41**, **43**, **50**), a sulfone (**37**), an alkene (**38**), an ester (**39**), carbamates (**44**, **46**, **47**), a ketal (**49**), and a ketone (**52**) were well accommodated in this convergent paired electrolysis. Moreover, various densely functionalized bioactive molecules such as 2,4-D (**53**), chlorambucil (**54**),

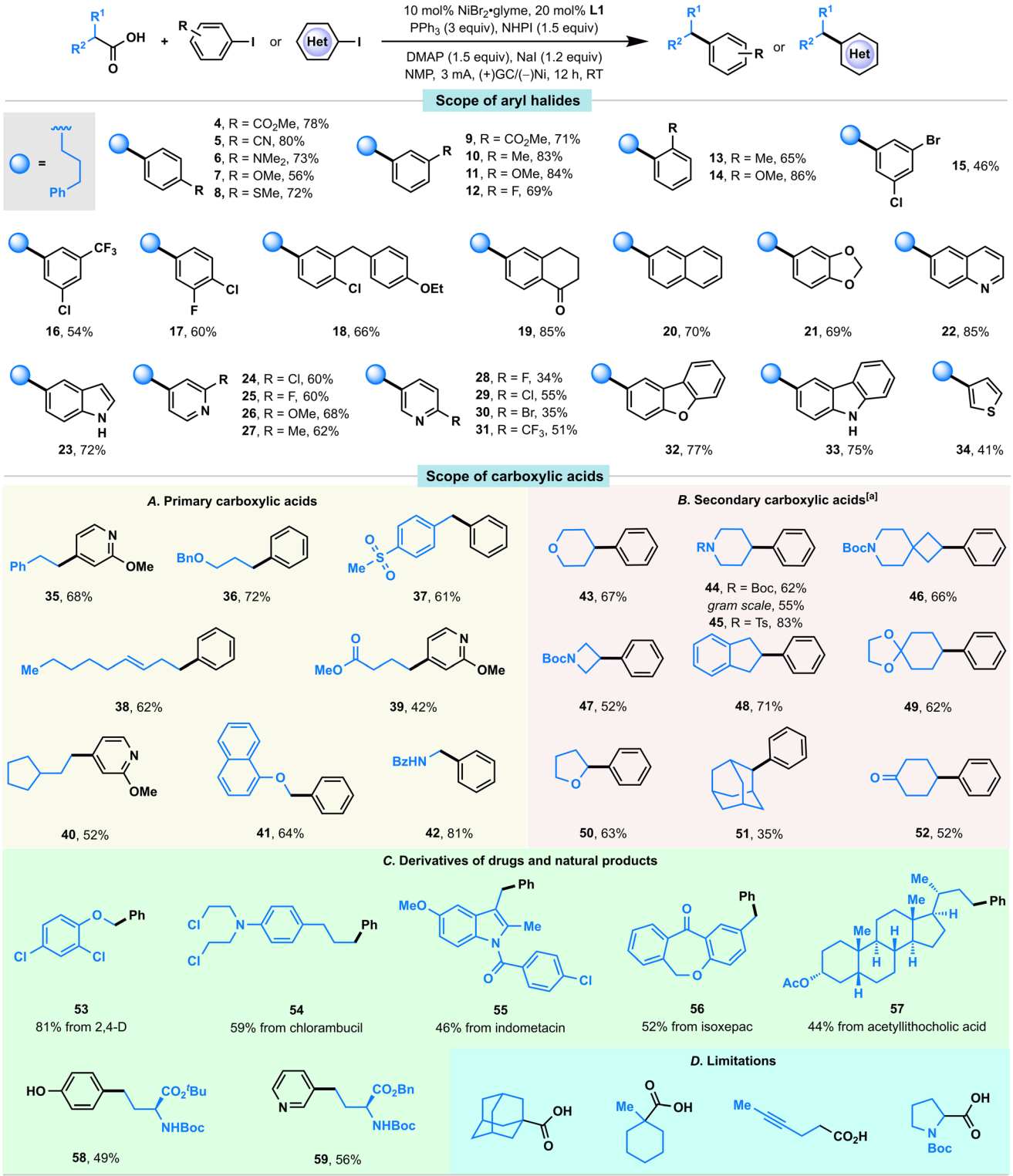

Fig. 2 Scope of the convergent paired electrolysis for decarboxylative arylation. Reactions were conducted on a 0.2 mmol scale; indicated yields are for isolated products. [a] The reactions were carried out with **L2**.

indometacin (**55**), isoxepac (**56**), and acetyllithocholic acid (**57**) could participate in this convergent paired electrolysis with high efficiency (Fig. 2C), supporting the applicability of our method for medicinal chemistry campaigns. Notably, the direct preparation of unnatural amino acids **58** (49%) and **59** (56%) from a protected glutamic acid showed comparable

efficiency observed in Baran's Ag–Ni electrocatalysis (59% NMR yield for **58**, 63% isolated yield for **59**; note that both were prepared from NHPI esters using a sacrificial Mg anode, 20 mol% Ni catalyst, and 50 mol% $AgNO_3$ in Baran's conditions),[5e] thereby demonstrating a novel approach to these synthetically challenging and highly valuable targets from simple starting materials. Note that: (i) the enantiomeric excess values of **58** and **59** were completely retained in our reaction conditions; (ii) this reaction could be performed on a gram scale (**44**).

In spite of the extensive success in coupling various aryl iodides and carboxylic acids, the existing reaction conditions face limitations in accommodating sterically hindered tertiary carboxylic acids, carboxylic acids with alkyne groups, or *N*-Boc-pyrrolidine (as illustrated in Fig. 2D). Additionally, it is noteworthy that a competition experiment, investigating diverse substituted carboxylic acids, revealed that primary carboxylic acids with comparatively lower steric hindrance exhibited higher reactivity than their more sterically hindered secondary counterparts (Fig. S4†).

Recently, Baran and co-workers developed a nickel-catalyzed electrochemical decarboxylative alkenylation of RAEs with vinyl iodides using Mg as the sacrificial anode and silver-nanoparticle-modified RVC as a cathode; this elegant electrolysis was used successfully in the preparation of a series of bioactive terpenes.[14] We also evaluated the ability of this paired electrolysis for decarboxylative alkenylation. To our delight, by simply switching the ligand from bpy **L1** to dtbpy **L2**, our protocol also showed comparable efficiency with Baran's method (Fig. 3), delivering natural products (*R*)-*E*-nerolidol (**62**), (*E*)-α-bisabolene (**63**), and a TBS-protected *E*,*E*-homofarnesol (**64**) with moderate-to-high yields directly from the corresponding acids.

Mechanistic studies

To unravel the intricate processes involved in this paired electrolysis, a comprehensive series of experiments was conducted to illuminate the entirety of the reaction mechanism. Initially, cyclic voltammetry (CV) experiments were undertaken, revealing that the electrolyte NaI exhibited the most facile oxidation (0.19 V *versus* Fc/Fc^+, in CH_3CN, Fig. 4B) within the santandard conditions. Notably, its oxidation potential was markedly lower than that of PPh_3, DMAP, NHPI, and carboxylic acid **1** (with oxidative potentials of 0.75, 0.95, 1.69, and 1.85 V *versus* Fc/Fc^+, respectively, in CH_3CN). This discrepancy strongly suggested that I_2 would be initially generated through anodic oxidation. Drawing parallels with the Appel reaction mechanism,[15] it was deduced that I_2 could rapidly react with PPh_3, yielding $PPh_3{\cdot}I_2$. This deduction was substantiated by the observable significant increase in the oxidation current of NaI in the presence of PPh_3 (red curve, Fig. 4B).

Given that the carboxylic acid **1** could be easily activated by the $PPh_3{\cdot}I_2$ to form an acyloxyphosphonium iodide, we postulated that this intermediate could react with NHPI in the presence of DMAP, yielding a NHPI ester.[9,11] Despite our efforts to isolate the NHPI ester of **1** by terminating the standard reaction prior to the complete consumption of **1**, our attempts proved unfruitful. We also employed ^{19}F NMR to detect the generation of the NHPI ester, utilizing carboxylic acid **65**; however, the corresponding NHPI ester **67** as not detected. We attribute this outcome to the low equilibrium concentration of the NHPI ester; the *in situ* generated NHPI ester is rapidly consumed under the net-redox-neutral conditions characteristic of the paired electrolysis. Recognizing the rapid consumption of the NHPI ester, we performed the electrolysis of carboxylic acid **66** in the presence of PPh_3, DMAP, and NaI first, followed by adding NHPI (without electric current at this stage), we successfully detected the NHPI ester **67** by ^{19}F NMR (Fig. S5†), thereby demonstrating its generation.

Having confirmed the NHPI ester was generated through an anodic oxidation, we next turned our attention to the cathodic reduction process. Notably, by using carboxylic acid **65**, we found that the rate of the consumption of carboxylic acid was highly dependent on the Ni catalyst loading (Fig. 4C). Specifically, the rate of carboxylic acid consumption accelerated proportionally with the increase in Ni catalyst loading. In the absence of the Ni catalyst, carboxylic acid exhibited a slow consumption rate, suggesting that the reduction of the *in situ* generated NHPI ester was predominantly catalyzed by Ni.

Our subsequent focus centered on the examination of nickel valence changes, and squarewave voltammetry (SWV, Fig. 4D) was used first to illustrate the reductive potentials of various Ni species. We found that: (i) the reductive potentials of **L1** ligated $NiBr_2$ and NiBr species were −1.59 V and −2.34 V, respectively (*versus* Fc/Fc^+ in NMP, represented by the black curve); (ii) the reductive potentials of the **L1** ligated Ni^{II}–aryl complex, generated *in situ* by oxidative addition of **L1** ligated $Ni(COD)_2$ to iodobenzene **2**, is −1.94 V (*versus* Fc/Fc^+ in NMP, represented by the blue curve); (iii) upon adding iodobenzene **2** to **L1** ligated $NiBr_2$, two additional peaks were detected (−1.72 V and −1.97 V, respectively, *versus* Fc/Fc^+ in NMP, represented by the red curve) before the reductive potential of **L1**

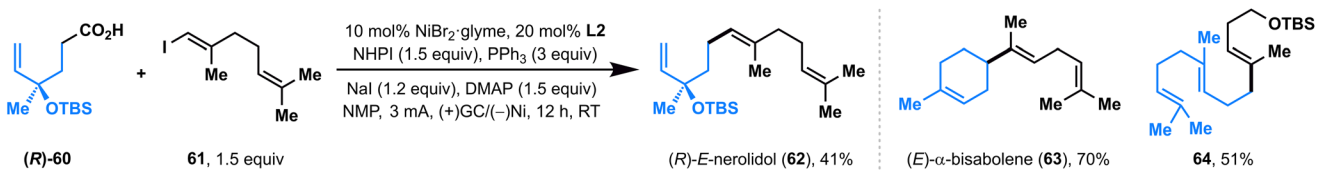

Fig. 3 The convergent paired electrolysis for the decarboxylative alkenylation.

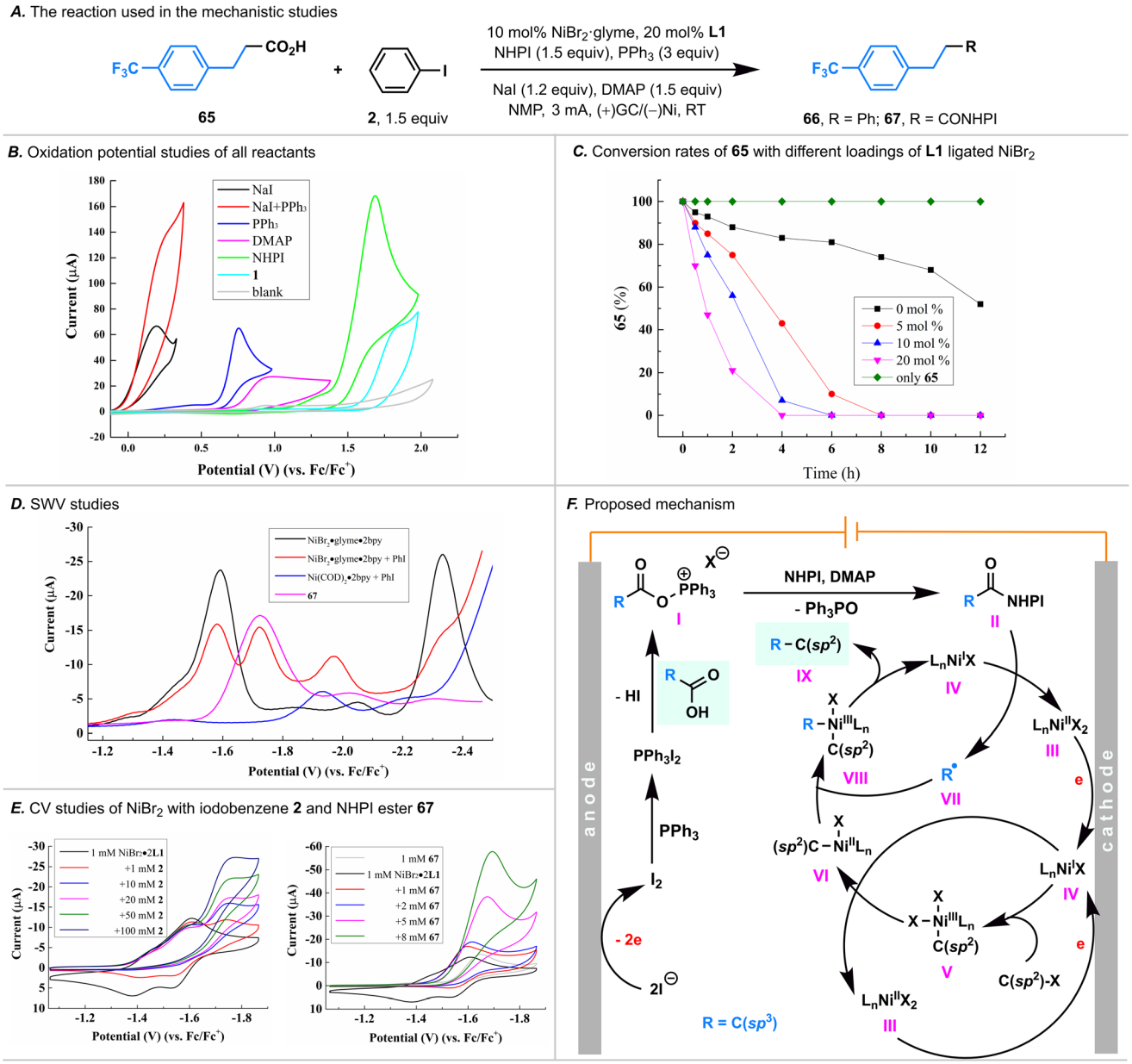

Fig. 4 (A) The reaction used in the mechanistic investigations. (B) Cyclic voltammetry (CV) studies for the anodic oxidation processes (1 mM with 0.1 M $LiClO_4$ in CH_3CN, ν = 100 mV s^{-1}, *versus* Fc/Fc^+). (C) Impact of the catalyst loading on the consumption rate of carboxylic acids **65**. Reactions were conducted on a 0.2 mmol scale; indicated yields were determined by ^{19}F NMR in $CDCl_3$ using $PhCF_3$ as the internal standard. (D) Squarewave voltammetry (SWV) studies of various **L1** ligated Ni species and **67** (1 mM with 0.1 M $LiClO_4$ in NMP, *versus* Fc/Fc^+) with an amplitude of 25 mV, frequency of 40 Hz, and a step potential of 5 mV. (E) CV investigation of **L1** ligated $NiBr_2$·glyme (1 mM with 0.1 M $LiClO_4$ in NMP, ν = 100 mV s^{-1}, *versus* Fc/Fc^+) with **2** or **67**. (F) Proposed mechanism for this convergent paired electrochemical decarboxylative arylation/alkenylation reaction.

ligated NiBr. Notably, the second peak (−1.97 V) being comparable to the reductive potential of the **L1** ligated Ni^{II}–aryl complex (−1.94 V) led us to hypothesize that the oxidative addition process of **L1** ligated NiBr to iodobenzene **2** occurred before the reduction of **L1** ligated NiBr to Ni^0, and the first peak (−1.72 V) is attributed to the reduction of the Ni^{III}–aryl complex to the Ni^{II}–aryl complex.

Subsequently, we employed CV experiments to substantiate our hypothesis (Fig. 4E). Firstly, the CV experiments showed that the reduction of **L1** ligated $NiBr_2$ to NiBr is reversible (represented by the black curve). Secondly, upon introducing iodobenzene **2** to the **L1** ligated $NiBr_2$, the reductive current peak of **L1** ligated $NiBr_2$ to NiBr is observed (−1.59 V *versus* Fc/Fc^+ in NMP), but the reversible peak disappeared (−1.54 V), indicating the consumption of **L1** ligated NiBr by iodobenzene **2** through an oxidative addition process. Thirdly, a reductive peak at −1.72 V was observed, consistent with the signal observed in SWV experiments. Notably, this peak exhibited

concentration-dependent increases in the reduction current, confirming the occurrence of the oxidative addition of **L1** ligated NiBr to iodobenzene. Furthermore, upon introducing the NHPI ester **67** to the **L1** ligated $NiBr_2$, the reoxidative current peak of **L1** ligated NiBr to $NiBr_2$ also disappeared, suggesting that the **L1** ligated NiBr could reduce the NHPI ester as well.

While further mechanistic investigations are warranted, our studies provide support for the proposed cathode-mediated Ni catalytic cycle (Fig. 4F). Firstly, Ni^{I} complex **IV** are preferentially generated from Ni^{II} species **III** *via* a cathodic reduction. Secondly, the oxidative addition of **IV** to iodobenzene generates Ni^{III}–aryl complex **V**, which undergoes reduction by Ni^{I} species **IV** through comproportionation, giving Ni^{II}–aryl complex **VI** and Ni^{II} species **III**.[16] **III** can obtain an electron from the cathode to reform Ni^{I} complex **IV**. Thirdly, by trapping an alkyl radical generated through the single electron reduction of NHPI ester by Ni^{I} species **IV**, Ni^{II}–aryl complex **VI** is converted to Ni^{III} adduct **VIII**, which, after reductive elimination, completes the cycle by producing the desired product **IX** and Ni^{I} complex **IV**. It is worth noting that while we cannot completely rule out the possibility that Ni^{III}–aryl complex **V** is directly reduced by the cathode to Ni^{II}–aryl complex **VI**, the similarity in reductive potentials between Ni^{III}–aryl complex **V** and NHPI ester (see Fig. 4D, −1.72 V *versus* Fc/Fc^{+}, in NMP) and the occurrence of homogeneous comproportionation between Ni^{III} and Ni^{I} favor the notion that Ni^{III}–aryl complex **V** is reduced by Ni^{I} species **IV**.

Conclusions

In conclusion, we have developed a convergent paired electrochemical decarboxylative arylation/alkenylation reaction by merging the anodic generation of RAEs and cathodic nickel-catalyzed reductive cross-coupling in an undivided electrochemical cell. This electrochemical cross-coupling reaction between alkyl carboxylic acids and $C(sp^2)$-iodides features exceptional substrate generality, high functional group compatibility, and mild reaction conditions, which have been well demonstrated with the successful preparation of synthetically challenging unnatural amino acids and terpenoid natural products. Detailed mechanistic studies demonstrated the *in situ* generation of NHPI esters *via* an anodic generated acyloxytriphenyl-phosphonium ion intermediate and the reductive cross-coupling mediated by the cathodic generated Ni^{I} species. Moreover, we anticipate that this convergent paired electrochemical strategy will serve as a powerful and flexible method for $C(sp^2)$–$C(sp^3)$ bond formation and is likely to find broad applications on account of its step and material economy.

Author contributions

C. Li, L. Li, and Z. Li conceived and designed the experiments. L. Li, Z. Li and W. Sun performed the experiments. The manuscript was written through contributions of all authors.

Conflicts of interest

The authors declare no competing financial interest.

Acknowledgements

Financial support for this research was provided by the MOST of China, and the Tsinghua Institute of Multidisciplinary Biomedical Research, Tsinghua University.

References

1 (*a*) G. Laudadio, M. D. Palkowitz, T. E.-H. Ewing and P. S. Baran, Decarboxylative Cross-Coupling: A Radical Tool in Medicinal Chemistry, *ACS Med. Chem. Lett.*, 2022, **13**, 1413–1420; (*b*) A. Y. Chan, I. B. Perry, N. B. Bissonnette, B. F. Buksh, G. A. Edwards, L. I. Frye, O. L. Garry, M. N. Lavagnino, B. X. Li, Y. Liang, E. Mao, A. Millet, J. V. Oakley, N. L. Reed, H. A. Sakai, C. P. Seath and D. W. C. MacMillan, Metallaphotoredox: The Merger of Photoredox and Transition Metal Catalysis, *Chem. Rev.*, 2022, **122**, 1485–1542; (*c*) J. Xuan, Z.-G. Zhang and W.-J. Xiao, Visible-Light-Induced Decarboxylative Functionalization of Carboxylic Acids and Their Derivatives, *Angew. Chem., Int. Ed.*, 2015, **54**, 15632–15641; (*d*) S. Murarka, *N*-(Acyloxy)phthalimides as Redox-Active Esters in Cross-Coupling Reactions, *Adv. Synth. Catal.*, 2018, **360**, 1735–1753; (*e*) T. Patra and D. Maiti, Decarboxylation as the Key Step in C–C Bond-Forming Reactions, *Chem. – Eur. J.*, 2017, **23**, 7382–7401; (*f*) S. K. Parida, T. Mandal, S. Das, S. K. Hota, S. D. Sarkar and S. Murarka, Single Electron Transfer-Induced Redox Processes Involving *N*-(Acyloxy)phthalimides, *ACS Catal.*, 2021, **11**, 1640–1683; (*g*) S. Karmakar, A. Silamkoti, N. A. Meanwell, A. Mathur and A. K. Gupta, Utilization of $C(sp^3)$-Carboxylic Acids and Their Redox-Active Esters in Decarboxylative Carbon—Carbon Bond Formation, *Adv. Synth. Catal.*, 2021, **363**, 3693–3736; (*h*) Y. Jin and H. Fu, Visible-Light Photoredox Decarboxylative Couplings, *Asian J. Org. Chem.*, 2017, **6**, 368–385; (*i*) H. Huang, K. Jia and Y. Chen, Radical Decarboxylative Functionalizations Enabled by Dual Photoredox Catalysis, *ACS Catal.*, 2016, **6**, 4983–4988.

2 (*a*) Z. Zuo, D. T. Ahneman, L. Chu, J. A. Terrett, A. G. Doyle and D. W. C. MacMillan, Merging Photoredox with Nickel Catalysis: Coupling of α-Carboxyl sp^3-Carbons with Aryl Halides, *Science*, 2014, **345**, 437–440; (*b*) A. Noble, S. J. McCarver and D. W. C. MacMillan, Merging Photoredox and Nickel Catalysis: Decarboxylative Cross-Coupling of Carboxylic Acids with Vinyl Halides, *J. Am. Chem. Soc.*, 2015, **137**, 624–627.

3 For selected examples using metal powders, see: (*a*) K. M. M. Huihui, J. A. Caputo, Z. Melchor, A. M. Olivares, A. M. Spiewak, K. A. Johnson, T. A. DiBenedetto, S. Kim, L. K. G. Ackerman and D. J. Weix, Decarboxylative Cross-Electrophile Coupling of *N*-Hydroxyphthalimide Esters with Aryl Iodides, *J. Am. Chem. Soc.*, 2016, **138**, 5016–5019; (*b*) D. C. Salgueiro;, B. K. Chi, I. A. Guzei, P. García-Reynaga and D. J. Weix, Control of Redox-Active Ester Reactivity Enables a General Cross-Electrophile Approach to Access Arylated Strained Rings, *Angew. Chem. Int. Ed.*, 2022, **61**, e202205673.

4 For selected examples using organic reducing agents, see: N. Suzuki, J. L. Hofstra, K. E. Poremba and S. E. Reisman, Nickel-Catalyzed Enantioselective Cross-Coupling of *N*-Hydroxyphthalimide Esters with Vinyl Bromides, *Org. Lett.*, 2017, **19**, 2150–2153.

5 For selected examples using electrochemical methods, see: (*a*) H. Li, C. P. Breen, H. Seo, T. F. Jamison, Y.-Q. Fang and M. M. Bio, Ni-Catalyzed Electrochemical Decarboxylative C–C Couplings in Batch and Continuous Flow, *Org. Lett.*, 2018, **20**, 1338–1341; (*b*) T. Koyanagi, A. Herath, A. Chong, M. Ratnikov, A. Valiere, J. Chang, V. Molteni and J. Loren, One-Pot Electrochemical Nickel-Catalyzed Decarboxylative Sp^2–Sp^3 Cross-Coupling, *Org. Lett.*, 2019, **21**, 816–820; (*c*) F. Lian, K. Xu, W. Meng, H. Zhang, Z. Tan and C. Zeng, Nickel-Catalyzed Electrochemical Reductive Decarboxylative Coupling of *N*-Hydroxyphthalimide Esters with Quinoxalinones, *Chem. Commun.*, 2019, **55**, 14685–14688; (*d*) Y. Liu, L. Xue, B. Shi, F. Bu, D. Wang, L. Lu, R. Shi and A. Lei, Catalyst-Free Electrochemical Decarboxylative Cross-Coupling of *N*-Hydroxyphthalimide Esters and N-Heteroarenes towards C(sp^3)–C(sp^2) Bond Formation, *Chem. Commun.*, 2019, **55**, 14922–14925; (*e*) M. D. Palkowitz, G. Laudadio, S. Kolb, J. Choi, M. S. Oderinde, T. E.-H. Ewing, P. N. Bolduc, T. Chen, H. Zhang, P. T. W. Cheng, B. Zhang, M. D. Mandler, V. D. Blasczak, J. M. Richter, M. R. Collins, R. L. Schioldager, M. Bravo, T. G. M. Dhar, B. Vokits, Y. Zhu, P.-G. Echeverria, M. A. Poss, S. A. Shaw, S. Clementson, N. N. Petersen, P. K. Mykhailiuk and P. S. Baran, Overcoming Limitations in Decarboxylative Arylation via Ag–Ni Electrocatalysis, *J. Am. Chem. Soc.*, 2022, **144**, 17709–17720.

6 For selected examples using photoreductant, see: L. M. Kammer, S. O. Badir, R.-M. Hu and G. A. Molander, Photoactive Electron Donor–Acceptor Complex Platform for Ni-Mediated C(sp^3)–C(sp^2) bond formation, *Chem. Sci.*, 2021, **12**, 5450–5457.

7 (*a*) K. Yang, J. Lu, L. Li, S. Luo and N. Fu, Electrophotochemical Metal-Catalyzed Decarboxylative Coupling of Aliphatic Carboxylic Acids, *Chem. – Eur. J.*, 2022, **28**, e202202370; (*b*) J. Lu, Y. Yao, L. Li and N. Fu, Dual Transition Metal Electrocatalysis: Direct Decarboxylative Alkenylation of Aliphatic Carboxylic Acids, *J. Am. Chem. Soc.*, 2023, **145**, 26774–26782.

8 Z. Li, W. Sun, X. Wang, L. Li, Y. Zhang and C. Li, Electrochemically Enabled, Nickel-Catalyzed Dehydroxylative Cross-Coupling of Alcohols with Aryl Halides, *J. Am. Chem. Soc.*, 2021, **143**, 3536–3543.

9 H. Ohmori, H. Maeda, M. Kikuoka, T. Maki and M. Masui, Electrochemical Generation and Reactions of Acyloxytriphenylphosphonium ions, *Tetrahedron*, 1991, **47**, 767–776.

10 For a recent review, see: Y. Wang, J. Xu, Y. Pan and Y. Wang, Recent Advances in Electrochemical Deoxygenation Reactions of Organic Compounds, *Org. Biomol. Chem.*, 2023, **21**, 1121–1133.

11 For selected examples, see: (*a*) A. Kumar, H. K. Akula and M. K. Lakshman, Simple Synthesis of Amides and Weinreb Amides Using PPh_3 or Polymer-Supported PPh_3 and Iodine, *Eur. J. Org. Chem.*, 2010, 2709–2715; (*b*) C. Duangkamol, S. Wangngae, M. Pattarawarapan and W. Phakhodee, Acyloxyphosphonium versus Aminophosphonium Intermediates: Application to the Synthesis of *N*-Acylbenzotriazoles, *Eur. J. Org. Chem.*, 2014, 7109–7112; (*c*) S. P. Morcillo, L. Á. de Cienfuegos, A. J. Mota, J. Justicia and R. Robles, Mild Method for the Selective Esterification of Carboxylic Acids Based on the Garegg-Samuelsson Reaction, *J. Org. Chem.*, 2011, **76**, 2277–2281; (*d*) N. Mamidi and D. Manna, $Zn(OTf)_2$-P romoted Chemoselective Esterification of Hydroxyl Group Bearing Carboxylic Acids, *J. Org. Chem.*, 2013, **78**, 2386–2396; (*e*) S.-P. Wang, C. W. Cheung and J.-A. Ma, Direct Amidation of Carboxylic Acids with Nitroarenes, *J. Org. Chem.*, 2019, **84**, 13922–13934.

12 For selected reviews on paired electrolysis, see: (*a*) N. Sbei, T. Hardwick and N. Ahmed, Green Chemistry: Electrochemical Organic Transformations via Paired Electrolysis, *ACS Sustainable Chem. Eng.*, 2021, **9**, 6148–6169; (*b*) J. C. Vantourout, From Bench to Plant: An Opportunity for Transition Metal Paired Electrocatalysis, *Org. Process Res. Dev.*, 2021, **25**, 2581–2586; (*c*) Y. Zhang, W. Sun and C. Li, Nickel-Catalyzed Paired Electrochemical Cross-Coupling of Aryl Halides with Nucleophiles, *Synthesis*, 2022, 281–294; (*d*) K.-J. Jiao, X.-T. Gao, C. Ma, P. Fang and T.-S. Mei, Recent Applications of Paired Electrolysis in Organic Synthesis, *Isr. J. Chem.*, 2023, e202300085; (*e*) R. Zhang, L. Li, K. Zhou and N. Fu, Radical-Based Convergent Paired Electrolysis, *Chem. – Eur. J.*, 2023, **29**, e202301034.

13 Building upon our prior investigation (ref. 8), it was established that a catalytic quantity of bromide ions, derived from $NiBr_2$, could serve as the initiator for the reaction, leading to the formation of $PPh_3{\cdot}Br_2$. In the present study, we posit that a catalytic quantity of bromide ion, originating from $NiBr_2$, also instigated the reaction. Furthermore, we propose that the liberation of the iodide ion from iodobenzene played a pivotal role in promoting the reaction.

14 S. J. Harwood, M. D. Palkowitz, C. N. Gannett, P. Perez, Z. Yao, L. Sun, H. D. Abruña, S. L. Anderson and P. S. Baran, Modular Terpene Synthesis enabled by Mild Electrochemical Couplings, *Science*, 2022, **375**, 745–752.

15 R. Appel, Tertiary Phosphane/Tetrachloromethane, a Versatile Reagent for Chlorination, Dehydration, and P–N Linkage, *Angew. Chem., Int. Ed. Engl.*, 1975, **14**, 801–811.

16 Y. Kawamata, J. C. Vantourout, D. P. Hickey, P. Bai, L. Chen, Q. Hou, W. Qiao, K. Barman, M. A. Edwards, A. F. Garrido-Castro, J. N. deGruyter, H. Nakamura, K. Knouse, C. Qin, K. J. Clay, D. Bao, C. Li, J. T. Starr, C. Garcia-Irizarry, N. Sach, H. S. White, M. Neurock, S. D. Minteer and P. S. Baran, Electrochemically Driven, Ni Catalyzed Aryl Amination: Scope, Mechanism, and Applications, *J. Am. Chem. Soc.*, 2019, **141**, 6392–6402.